Antiprotonic Radioactive Atom for Nuclear Structure Studies

M. Wada* and Y. Yamazaki*,†

*Atomic Physics Laboratory, RIKEN 2-1 Hirosawa, Wako, Saitama 351-0198, Japan
† Institute of Physics, Graduate School of Arts and Sciences, University of Tokyo, 3-8-1, Komaba, Meguro, Tokyo 153-8902, Japan

Abstract. A future experiment to synthesize antiprotonic radioactive nuclear ions is proposed for nuclear structure studies. Antiprotonic radioactive nuclear atom can be synthesized in a nested Penning trap where a cloud of antiprotons is prestored and slow radioactive nuclear ions are bunch-injected into the trap. By observing of the ratio of π^+ and π^- produced in the annihilation process, we can deduce the different abundance of protons and neutrons at the surface of the nuclei. The proposed method would provide a unique probe for investigating the nuclear structure of unstable nuclei.

Keywords: antiprotonic atom, nuclear structure, neutron halo, radioactive beam
PACS: 29.25.Rm 41.85.Ar 21.10.Gv 25.43.+t 36.10.-k

INTRODUCTION

Exotic properties of nuclei, such as halo and skin, have been investigated in nuclei far from the stability line [1]. Various experimental methods have been applied or proposed to investigate the nuclear size and form of unstable nuclei as listed in Table 1. Precision optical spectroscopy have been used to determine the charge radii of many unstable nuclei. Bohr-Weisskopf effect [2], which can be derived by precision hyperfine structure spectroscopy, is sensitive to the distribution of magnetism in a nucleus (DNM). Muonic X-ray measurement is more sensitive to the nuclear volume effect in such atomic spectroscopy. Although the short lifetime of muons makes experiments difficult, a new experimental scheme for unstable nuclei was proposed and tested with some stable nuclei [3]. Electron elastic scattering is an ideal probe to determine nuclear form factors; however, the small cross section has limited its applications to unstable nuclei. Recently, a new scheme—SCRIT (self-confining radioactive isotope target)—where unstable nuclear ions are trapped in an electron beam was proposed for electron scattering experiments for unstable nuclei [4]. We expect to obtain accurate charge radii and charge form factor of some unstable nuclei using such new experimental methods based on the electromagnetic interaction at the new radioactive ion beam facilities.

The most successful experiment to investigate the halo structure of unstable nuclei is the interaction cross section measurement in the nuclear fragmentation reaction of intermediate-energy radioactive nuclear beams [5]. Although a nuclear model is required to determine the matter radii of nuclei, many exotic nuclei have been investigated by this highly sensitive experimental method. The distribution of nuclear matter can be measured by proton elastic scattering wherein solid hydrogen can be used as the target

CP793 *Physics with Ultra Slow Antiproton Beams*
edited by Yasunori Yamazaki and Michiharu Wada

TABLE 1. Experimental methods for determining the nuclear size and form of unstable nuclei, based on the electro-magnetic (top) and the strong (bottom) interactions.

Method	Quantity	For RIB	
Optical spectroscopy (IS)	$\langle R^2_{\rm charge}\rangle^{1/2}$ (Relative)	Possible ($> 10^2$/s)	Many unstable nuclides of good elements. Only sensitive to protons.
Microwave spectroscopy (hfs)	$\langle R^2_{\rm mag}\rangle^{1/2}$ (Relative)	Possible (10^2 in trap)	Bohr-Weisskopf effect (DNM), Only for a few elements such as alkaline-earth.
Muonic X-ray	$\langle R^2_{\rm charge}\rangle^{1/2}$, $\langle R^2_{\rm mag}\rangle^{1/2}$ (Absolute)	[3] (10^9 atoms)	Absolute charge radii, DNM, short $T_{1/2}$ of μ limits possible nuclides
Electron scattering	$\rho_{\rm c}(r), (\rho_{\rm mag}(r))$	[8] ($> 10^6$ atoms)	Charge and magnetic form factors, universal electro-magnetic probe. Small cross section limits possible nuclides
Interaction cross section	$\langle R^2_{\rm matter}\rangle^{1/2}$	Possible (0.01/s)	Nuclear matter size. Model is required to determine nuclear rms radii.
Proton elastic scattering	$\rho_{\rm matter}(r)$	Possible (10^3/s)	Nuclear matter distribution. Model is required.
Antiproton scattering	$\langle R^2_{\rm p}\rangle^{1/2}, \langle R^2_{\rm n}\rangle^{1/2}$	Possible [7]	Independent determination of proton & neutron rms radii.
Antiprotonic atom	$\frac{\rho_{\rm p}}{\rho_{\rm n}}\vert_{\rm surface}$	Possible ($> 10^3$/s)	Different abundances of of protons and neutrons at nuclear surface.

and an intermediate-energy radioactive ion beam hits the target. Using this scheme even very short-lived nuclei, i.e., $T_{1/2} < 1$ ms, can be investigated.

Recently, two new experiments for unstable nuclei using antiproton were proposed [6, 7]. One is the antiproton ion collision experiment in a storage ring; in this experiment, the absorption cross section of an antiproton by a nucleon of the unstable nucleus is measured at intermediate energy. Since particle identification of the residual nuclei allows us to distinguish proton absorption events and neutron absorption events, the root mean square radii of protons and neutrons in the nucleus can be determined independently. The other experiment is the antiprotonic radioactive atom experiment, which is discussed in this paper.

Different abundances of protons and neutrons at the surface of the nuclei are an important concern for nuclear structure studies. Antiprotonic atoms would be excellent probes for such different nucleon abundance at the surface; this is because annihilation of an antiproton dominantly occurs with a nucleon at the surface of a nucleus and the vanished nucleon can be identified by the total charge of the emitted pions or the residual nucleus.

Antiprotonic atoms have been studied exclusively for stable nuclei by using various experimental methods as shown in Table 2. Antiprotonic atoms were produced by irradiating an antiproton beam on a fixed target material. When an antiproton is captured in an electronic orbital of an atom, it decays to lower levels by radiating Auger electrons and X-rays. The lowest X-ray transition level indicates the matter radius of the nucleus [9]. At a certain level where a sizeable overlapping of the wavefunctions of the antiproton

TABLE 2. Experimental methods for antiprotonic atom and obtainable physical quantities

Physical quantity	Observable	Method	For RIB	previous studies
Nuclear size	X-ray			Trzcinska et al [9]
p, n abundance at nuclear surface	Pion's net charge	Calorimetric		Bugg et al [10]
		Statistical	Possible	
	Cold residue	γ-ray		Jastrzebski et al [11]
		Recoil momentum	Possible	
Surface nucleon's momentum	Cold residue	Recoil momentum	Possible	

and the nucleons exists, annihilation occurs between the antiproton and a nucleon of the nucleus. The implication of these studies is that the annihilation dominantly occurs with a nucleon at the surface of the nucleus and that it can be determined whether the vanished nucleon is a proton or a neutron based on the following phenomena. One is that $\bar{\text{p}}$-n and $\bar{\text{p}}$-p annihilations produce charged pions with a net charge of -1 and 0, respectively. Bugg et al. used a bubble chamber to detect charged pions and identified the annihilated nucleons [10]. The other is the fact that the "cold" residual nucleus ${}^{A}_{N}Z$ becomes ${}^{A-1}_{N-1}Z$ and ${}^{A-1}_{N}(Z-1)$, as consequences of $\bar{\text{p}}$-n and $\bar{\text{p}}$-p annihilations, respectively. The Warsaw group detected γ-rays to identify the cold residues [11].

An important advantage of the pion detection method is its universality. In particular, when nuclei close to the drip line are concerned, other methods are often inapplicable. One or both of residual nuclei, ${}^{A-1}_{N-1}Z$ and ${}^{A-1}_{N}(Z-1)$, often become particle-unbound nuclei. Pions can be observed even if the residual nucleus does not exist.

FORMATION AND DETECTION OF ANTIPROTONIC RADIOACTIVE ATOMS

All the previous experiments used a fixed target and a fast antiproton beam. However, such methods are impossible to be applied to radioactive nuclei since the number of radioactive nuclei is always much smaller compared to that of stable nuclei and they decay within finite lifetimes. The sensitivity of the detection methods should also be high for such a limited number of radioactive species. In our proposal, therefore, we use a cloud of antiprotons trapped in a Penning trap as the target and singly ionized slow radioactive nuclear ions as projectiles [6]. Figure 1 shows a schematic potential diagram of the nested Penning trap. In this figure, negatively charged antiprotons are confined in a positive well at the center of a nested trap while positively charged slow ions are bunch-injected into the negative outer well of the trap.

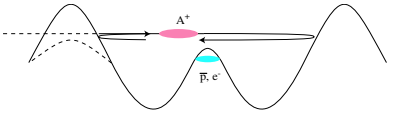

FIGURE 1. Potential diagram of the nested Penning trap for the $\bar{\text{p}}$-RI atom.

Among several detection schemes, statistical analysis of the ratio of the detected π^+ to π^- is the most feasible and universal method for antiprotonic radioactive atoms. The detection efficiency for γ-rays is much lower than that for charged pions and the radiochemical method is not effective for nuclei close to the drip line. The detection of X-rays enables us to investigate the matter radii of nuclei, however, the detection efficiency is also limited if all possible geometries are considered. Furthermore, the matter radii can be measured quite easily, for instance, by the measurements of the total interaction cross sections in intermediate energy reactions. The particle identification of recoiling residual nuclei is also a potential method for antiprotonic radioactive atoms. Details of the detection scheme will be discussed in a later section. Here, we focus on the detection of charged pions, so far.

Production rate

The antiproton capture cross sections of slow singly charged ions were theoretically estimated by Cohen [12] and they are as large as those of neutral atoms (Fig. 2). A typical value is 4×10^{-16} cm^2 for ^{11}Li$^+$ ions when the relative energy is 0.1 atomic units which corresponds to a ^{11}Li$^+$-beam energy of 33 eV in the antiproton rest frame. Assuming that the number of trapped antiprotons is 5×10^6 [13] and that they are confined within 1 mm^2, the target density is $N(\bar{\mathrm{p}}) = 5\times10^8$ cm^{-2}. Slow RI ions are bunch-injected into a nested trap and they pass through the antiproton cloud for 5×10^5 s^{-1} if the ions are 33-eV ^{11}Li$^+$ and the trap length is 4 cm. Since we are mainly interested in very short-lived nuclei, we assume a short measurement cycle of 10 ms, in which only 10 RI ions are involved when the RI beam intensity is 10^3 s^{-1} . Then, the production rate per cycle is $Y = 4\times10^{-16}\cdot5\times10^8\cdot10\cdot5\times10^3 = 1\times10^{-2}$. Thus, in total one antiprotonic- ^{11}Li^{++} ion can be produced per second. This is quite a feasible number.

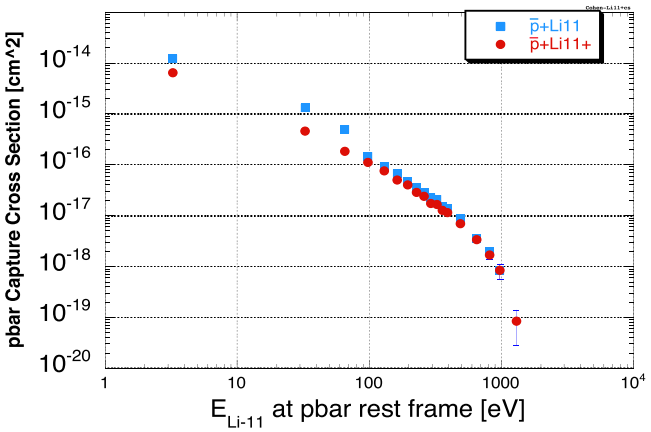

FIGURE 2. Theoretically evaluated capture cross section of antiproton in Li$^+$ ion and neutral atom [12].

Detector setup

The purpose of the detectors is to identify the polarity of the charged pions from annihilation events. A stack of position sensitive detectors (PSDs) cylindrically covers the nested trap in order to track the path of the charged pions. The polarity can be deduced from the deflection direction in a high magnetic field ($\sim$5 T) and noise events from the annihilations that are not caused in the center of the trap can be discriminated. For the charged pions with an energy between 100 MeV to 400 MeV, the curvatures of the paths under 5 T are $\sim$100 to $\sim$200 mm. If three layers of detectors are located 10 mm apart from one another, the position at the central layer is shifted by more than 0.5 mm from the other two layers. A relatively simple PSD can be used for this purpose and several types of detectors are candidates—silicon PSD, multi-wire gas counter, fiber scintillators and so on.

Discrimination of the background events is an important concern for the detector setup. The major background events are: 1) energetic protons directly emitted from the annihilated nucleus, 2) γ-rays due to uncharged pions and X-rays from cascade, and 3) pions produced in the annihilation events with background gas. Protons and γ-rays can be discriminated by the response of the detectors and also by the curvature of the paths in the tracking detectors. Note that the multiplicity of direct proton event is as small as one [14]. Pions originating to the background gas would have the biggest effect, since 10^7 antiprotons in a trap with a long storage lifetime of one day already annihilate at a rate of 100 Hz, which is much higher than the expected true event rate. However, the residual gas is almost purely H_2 at cryogenic temperature, i.e., such an annihilation does not produce any recoil nuclei. If we detect a recoil nucleus coincident with pions, we can clearly identify a true event. Figure 3 shows the detection efficiencies of recoil ions obtained by using a detector with a diameter of 40 mm located at a distance of 400 mm from the center of the trap under a magnetic field of 5 T. Even if the solid angle is as small as 0.06%, high efficiencies are expected—especially for heavier ions—due to the presence of the strong magnetic field.

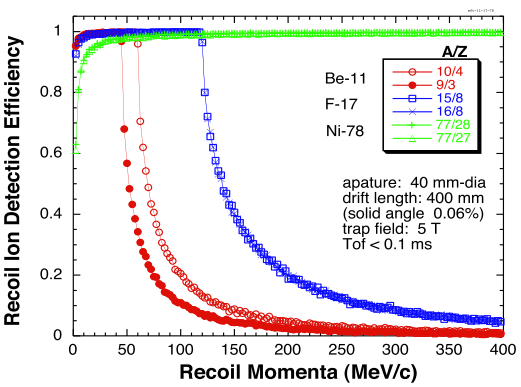

FIGURE 3. Detection efficiencies of recoil ions from annihilation events.

The detector of recoil ions can be used not only to eliminate background events but also to identify the recoil particles, if the position of the detected ions in the recoil ion detector and the position of the annihilation point are accurately measured. The relation of the longitudinal distance between the two positions, L, and the radial distance between the two positions, d, is expressed as

$$d = 2\frac{m}{qB}\sqrt{\frac{2E}{m}\left(\frac{L}{tof}\right)^2}\left|\sin\left(\frac{qB}{2m}tof\right)\right| \tag{1}$$

where E is the kinetic energy of ions; m, mass; q, charge; B, magnetic field and tof, time-of-flight. Here we see that even the kinetic energy of recoil ion can be determined from the measured quantities. However, it should be noted that accurate measurement of the annihilation position to determine the kinetic energy is difficult by means of the present technique. Further development is required for this particular purpose.

SIMULATION AND ANALYSIS

The simplest statistical analysis of the pion detection method is to compare the ratio of the total numbers of detected π^- and π^+ throughout a measurement. This yields the nucleon density ratio $\rho(\mathrm{n})/\rho(\mathrm{p})$ at the surface of a nucleus, $R_{\mathrm{n/p}}$, even if the detection efficiency of charged pions is low. Note that if all the charged pions can be detected, a single event can determine the net charge of an annihilation event; therefore $\bar{\mathrm{p}}$-n or $\bar{\mathrm{p}}$-p annihilation events can be distinguished each other. However, the detection efficiency cannot be unity in usual cases. A simulation (Fig. 4) shows that the nucleon density ratio at the surface $R_{\mathrm{n/p}}$ can be obtained with a 5% accuracy from 5×10^5 antiprotonic atoms.

If the detection efficiency is reasonably high, the multiplicity of detected charged pions (M) and their total charge per event (Σ_c) can be measured; this provides useful infor-

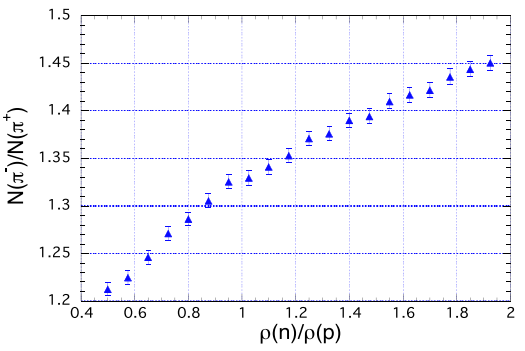

FIGURE 4. Simulated ratio of the total number of π^- to that of π^+ plotted as function of $R_{\mathrm{n/p}}$. The error bar shows the statistical error when 5×10^5 antiprotonic atoms are formed and charged pions produced by annihilation are detected with a 50% efficiency.

TABLE 3. Simulated histogram of the multiplicity of charged pions (row) and the total charge per event (column) under a typical experimental condition: $R_{\mathrm{n/p}} = 1.0$, $\varepsilon_+ = \varepsilon_- = 0.6$, $\omega_+ = \omega_- = 0.1$, $\lambda_+ = \lambda_- = 0.1$. The number of total annihilation event is 10^5.

$M\backslash\Sigma_c$	-5	-4	-3	-2	-1	0	+1	+2	+3	+4	
0	0	0	0	0	0	0	0	0	0	0	(11386)*
1	0	0	0	0	17223	0	11233	0	0	0	28456
2	0	0	0	7530	0	21437	0	2844	0	0	31811
3	0	0	1029	0	11901	0	6591	0	179	0	19700
4	0	44	0	1904	0	4394	0	519	0	5	6866
5	1	0	99	0	979	0	451	0	13	0	1543
6	0	2	0	75	0	133	0	14	0	0	224
7	0	0	1	0	7	0	3	0	0	0	11
8	0	0	0	1	0	1	0	0	0	0	2
9	0	0	0	0	1	0	0	0	0	0	1
	1	46	1129	9510	30111	25965	18278	3377	192	5	88612

* unobservable events

mation [15]. The observation probabilities of charged pions are functions of the charge of annihilated nucleons, the initial multiplicities of $\pi^{0,\pm}$, the absorption or charge exchange probabilities ($\omega_\pm$) of $\pi^\pm$ by the residual nucleus, the charge exchange probabilities ($\lambda_\pm$) of π^0, and the detection efficiencies ($\varepsilon_\pm$). The double charge exchange probabilities can be ignored. Assuming 60% detection efficiencies of charged pions and other relevant experimental parameters, observed events are simulated and histogrammed in terms of M and Σ_c (Table 3). The initial multiplicities of $\bar{\mathrm{p}}$-p and $\bar{\mathrm{p}}$-n annihilations are obtained from literature [16].

The count distribution of each cell depends not only on $R_{\mathrm{n/p}}$ but also on $\varepsilon_\pm$, $\omega_\pm$, and $\lambda_\pm$. If these parameters are sufficiently orthogonal to each other, they can be obtained by fitting the measured values like Table 3. While $\varepsilon_\pm$ and $\omega_\pm$ are strongly correlated, $R_{\mathrm{n/p}}$ and $\lambda_\pm$ cause reasonably independent effect to the values of the histogram. Figure 5 is an example simulation result of their dependences. Here, we evaluate only the projected histograms of M and Σ_c, which correspond to the rightmost column and the bottom row of Table 3—not each cell of the table. Evidently, M has small dependence on $R_{\mathrm{n/p}}$ while Σ_c is strongly dependent on $R_{\mathrm{n/p}}$. Increases in λ_- and ω_+ or decreases in λ_+ and ω_- cause a similar global effect of lowering the average charge; however, the trend of each values shows a different dependence.

EXPERIMENTAL LOCATIONS

The proposed experiment requires the simultaneous availability of slow radioactive nuclear beams and trapped antiprotons. To date, a large number of trapped antiprotons have only been available at the CERN antiproton decelerator facility (AD). If a beam transport line can be build from CERN ISOLDE to AD, it can be a possible location for the experiment proposed in this study. The other possibility at CERN is to bring trapped antiprotons from AD to ISOLDE by using a portable trap. In this scheme, a long beam transport line for slow RI-beams from ISOLDE is not needed. On the other hand, if such

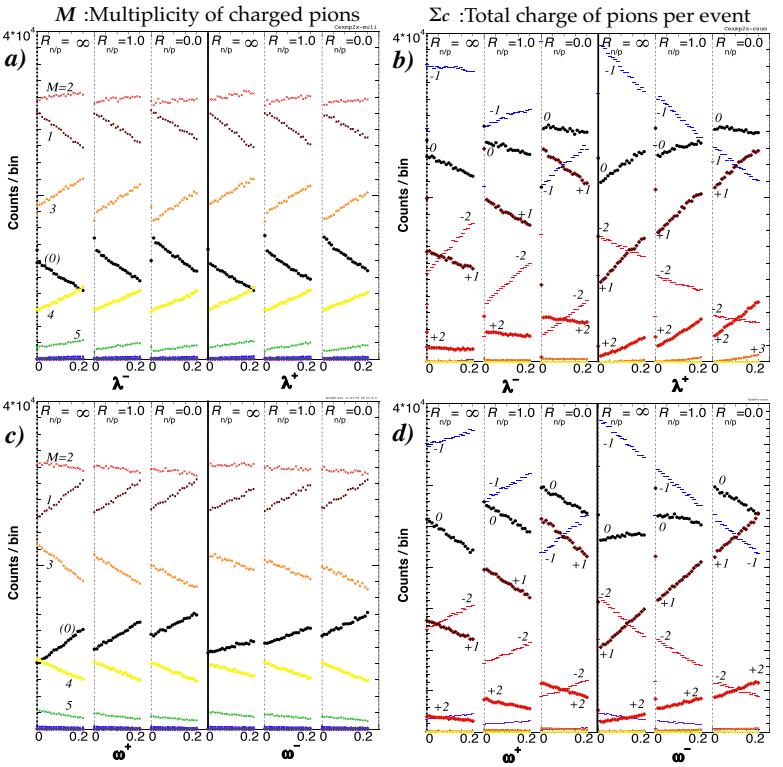

FIGURE 5. Simulation of the dependence of the detected charged pion's multiplicity (left (a, c)) and the total charge per event (right (b, d)) on the charge exchange probability $\lambda_{\pm}$ (top (a, b)) and on the absorption probability $\omega_{\pm}$ (bottom (c, d)). For a) and b), λ_{-} and λ_{+} are scanned from 0.0 to 0.2 while the other parameters are fixed: $\varepsilon_{\pm} = 0.6$, $\omega_{\pm} = 0.1$ and $\lambda_{+} = 0.1$ for the three left scans ($\lambda_{-} = 0.1$ for the three right scans). For c) and d), ω_{+} (three left scans) and ω_{-} (three right scans) are scanned from 0.0 to 0.2 when $\lambda_{\pm} = 0.1$. $R_{\mathrm{n/p}}$ is set for three extreme cases: ∞ (neutron only), 1.0 (equal distribution) and 0.0 (proton dominant).

a portable trap is realized for antiprotons and the trapping lifetime is sufficiently long, trapped antiprotons can be brought to RI beam facilities around the world. One candidate is SLOWRI at RIKEN RIBF [17]. This facility in Japan, which is under construction, aims to provide slow and trapped RI beams of thousands of unstable isotopes of all atomic elements using a superconducting heavy ion cyclotron, the projectile fragment separator BigRIPS, and an RF ion guide. One of the planned experiments at SLOWRI is $\bar{\mathrm{p}}$-RI. Since the trapping lifetime of the portable trap must be more than one week, technical evaluation of the vacuum technologies for such a trap is currently being done. As regards other future facilities, FAIR at GSI is an important candidate. This facility will provide us trapped antiprotons at FLAIR, and the low-energy branch of NUSTAR will provide us universal slow RI beams. Thus we propose antiprotonic radioactive atom

experiments at the FAIR project by the Exo+pbar collaboration.

CONCLUSION

Antiprotonic radioactive nuclear atoms would be new and unique probes for nuclear structure studies of unstable nuclei. Among several experimental schemes of antiprotonic atoms, the pion detection method is advantageous in terms of the universality and richness of the obtainable information. Charged pion emissions followed by annihilation are observable even if the residual nuclei are unbound or fragmented. The statistically acquired matrix of the charged pion multiplicity M and the total charge per event Σ_c allows us as to fit not only for the different distributions of protons and neutrons at the nuclear surface, $R_{n/p}$, but also the pion absorption probabilities $\omega_{\pm}$ and the charge exchange probabilities $\lambda_{\pm}$. The experimental technologies in the detectors and the trap should be improved further in order to realize the proposed experiments in the coming decade.

ACKNOWLEDGMENTS

This report describes the proposed experiments by the SLOWRI collaboration at RIKEN RIBF and by the Exo+pbar collaboration for the GSI-FAIR project. The authors acknowledge the members of these two collaborations, especially, Prof. Wycech for helpful discussions.

REFERENCES

1. I. Tanihata, et al., *Phys. Rev. Lett.* **55** (1985) 2676.
2. A. Bohr and V. F. Weisskopf, *Phys. Rev.* **77** (1950) 94.
3. P. Strasser, these proceedings.
4. W. Wakasugi, T. Suda and Y. Yano, *Nucl. Instr. Meth.* **A532** (2004) 216.
5. T. Ozawa, these proceedings.
6. M. Wada and Y. Yamazaki, *Nucl. Instr. Meth.* **B214** (2004) 196.
7. P. Kienle, these proceedings.
8. T. Suda, these proceedings.
9. Trzcinska et al., *Phys. Rev. Lett.* **87** (2001) 82501.
10. W. M. Bugg, G. T. Condo, E. L. Hart, H. O. Cohn and R. D. McCulloch, *Phys. Rev. Lett.* **31** (1973) 475.
11. Jastrzebski et al., *Nucl. Phys.* **A588** (1993) 405c.
12. J. S. Cohen, *Phys. Rev.* **A 69** (2004) 022501.
13. N. Kuroda, H. A. Torii, K. Yoshiki Franzen, Z. Wang, S. Yoneda, M. Inoue, M. Hori, B. Juhasz, D. Horvath, H. Higaki, A. Mohri, J. Eades, K. Komaki and Y. Yamazaki, *Phys. Rev. Lett.* **94** (2005) 023401.
14. D. Polster et.al, *Phys. Rev.* **C51** (1995) 1167.
15. S. Wycech, these proceedings.
16. J. Riedlberger et. al, *Phys. Rev.* **C**40(1989) 2717.
17. M. Wada, Y. Ishida, T. Nakamura, Y. Yamazaki, T. Kambara, H. Ohyama, Y. Kanai, T. M. Kojima, Y. Nakai, N. Ohshima, A. Yoshida, T. Kubo, Y. Matsuo, Y. Fukuyama, K. Okada, T. Sonoda, S. Ohtani, K. Noda, H. Kawakami and I. Katayama, *Nucl. Instr. Meth.* **B204** (2003) 570.